LASER-PLASMA BASED ELECTRON ACCELERATION EXPERIMENTS: STATUS IN INDIA

P. A. Naik [#], B. S. Rao, A. Moorti, and P. D. Gupta, RRCAT, Indore, India

Abstract

Experiments on laser-plasma based electron acceleration using a table-top 10 TW laser system were initiated in India at Laser Plasma Division, RRCAT, in November 2006. Significant progress has been made since then in terms of understanding the effect of various laser-plasma interaction conditions on laser-driven acceleration and improving the electron beam quality. During the experimental studies, we were able to produce quasi-monoenergetic electron beam in the energy range of 10 – 50 MeV, with divergence ~ 3 - 7 mrad, from helium gas-jet plasma. The laser pulse parameters were found to influence propagation of the high power laser beam in plasma and also the parameters of the electron beam.

INTRODUCTION

Laser-driven plasma-based accelerator offers accelerating electric field larger than 100 GV/m [1], which is more than thousand times higher than that possible in a conventional RF based accelerator. Therefore, it is a promising method to reduce the size of the present day RF-cavity based TeV energy electron accelerators from kilometers to few meters. Such a significant reduction in size can make the construction of a table-top size electron accelerators feasible and affordable by smaller laboratories in future. Recent experiments on laser-plasma based electron accelerators have demonstrated good quality relativistic electron beams with energy up to GeV energy over centimeter acceleration length, in a compact set-up [2]. However, there remains a need to identify the range of laser and plasma parameters over which stable mono-energetic electron beams are produced. As the stability and physics of electron beam acceleration may be affected by the laser beam propagation and associated processes in the plasma, it is necessary to study the effect of various parameters (e.g. laser focusing, laser chirp, and laser pre-pulse) on the electron acceleration and its stability.

Experiments were carried out using the 45 fs, 10 TW Ti:sapphire laser system at RRCAT, which can operate from single-shot mode to 10 Hz rep-rate. Electron acceleration was demonstrated using this laser in the initial experiment [3] which was carried out in collaboration with KEK, Japan, Subsequently, more detailed studies were carried out independently and various interesting features were found, leading to production of a well-collimated, mono-energetic electron beam. We have found that the laser-pulse parameters play a critical role in the stable propagation of the intense laser beam in plasma, which in turn affects the electron beam acceleration. In this paper, we shall discus these experiments in detail and present the status.

[#]panaik@rrcat.gov.in

EXPERIMENTAL SETUP

The basic experimental setup used for laser-plasma based electron acceleration is shown in Fig. 1. The Ti:sapphire table-top terawatt laser at Laser Plasma Division, RRCAT, was used for the experiment. The laser system provides horizontally polarized, 45±5 fs duration pulses with maximum 10 TW peak power. The central wavelength (λ_o) of the laser is at 790 nm and the FWHM bandwidth ($\Delta\lambda$) is 20 nm. The laser beam was focused on a helium gas-jet target using either f/10 or f/7.5 gold-coated off-axis parabolic mirror (OAPM), to a spot of size of 18 μm or 10 μm (FWHM) with Rayleigh lengths 300 μm and 130 μm respectively. The intensity of the laser on target was $1.2\text{x}10^{18}$ W/cm^2 and $2.4\text{x}10^{18}$ W/cm^2 respectively for f/10 and f/7.5 focusing conditions. The contrast ratio of the pre-pulse before 8 ns was better than 10^6 and the contrast ratio of ns-pedestal due to amplified spontaneous emission (ASE) was also about 10^6. The length of the ASE pedestal was controlled by changing the switching time of the pulse cleaner (Pockels cell) after the regenerative amplifier. A rectangular (dimensions: 1.2 mm x 10 mm) slit type Laval nozzle [4] was used to produce supersonic gas jet in pulsed mode with ~ 2 ms opening duration. The laser beam was focused at a height of about 1 mm from the exit of the slit nozzle. The backing pressure of the gas-jet was varied to provide helium gas density in the range of n_{gas} ~ 1 to 5 x 10^{19} cm^{-3} in the interaction region. As the helium gas gets fully ionized by the foot of the fs-laser pulse (at an intensity of ~ 10^{16} W/cm^2), the electron density (n_e), during the

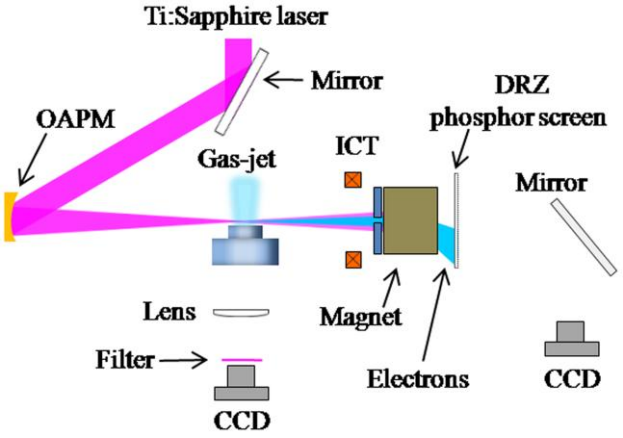

Figure 1: Schematic of the basic experimental setup used for laser-plasma based electron acceleration

interaction of the main intense portion of the laser pulse, would be twice the initial gas density. The main diagnostics used to characterize the accelerated electron beam were : an integrating current transformer (ICT-082-070-5:1) to measure the total electron beam charge, and a phosphor screen combined with CCD imaging, for electron beam profile monitoring. A single-shot electron spectrometer was set up using two circular (ϕ = 50 mm) permanent magnets (B_{eff} = 0.46 T) with pole gap of 9 mm to measure the energy of the accelerated electrons. 90^o Thomson scattering radiation at 90^o to the laser propagation axis was collected to record the magnified images of the laser guiding in the plasma imaged using a 12-bit CCD camera.

RESULTS AND DISCUSSION

In this section, we will present and discuss the results of two recent experiments performed with different laser focusing conditions. In both the experiments, the accelerated electrons were produced for gas density more than well defined threshold that depended on the f-number (i.e. ratio of focal length of the optics and beam diameter) of the OAPM used. The integrated charge of the electron beam in both focusing conditions was measured to be few nC. The electron beam profile was found to be sensitive to the gas density. In both the cases, a well collimated electron beam with divergence < 10 mrad was produced, but at different gas densities. The well collimated electron beam in the case of f/7.5 OAP was produced at ~ 3x10^{19} cm^{-3} while in the case of f/10 OAP it was at ~ 4x10^{19} cm^{-3}. In both the experiments, the laser power was higher than the critical power for relativistic self-focusing. The forward scattered laser spectrum in the case of f/10 focusing consisted of clear Raman satellites as shown in Fig. 2(a). This indicates the self-modulation of the laser pulse and its role on electron acceleration [5]. The well collimated electron beam in the case of f/10 consists of background electrons with large divergence and > 5 MeV energy as shown in Fig. 2(b). Note that the image in Fig. 2(b) was recorded with thick

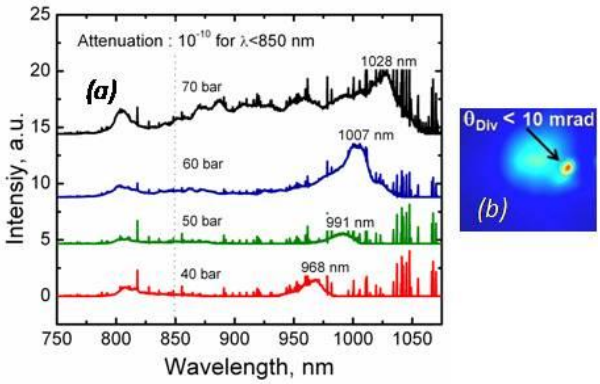

Figure 2: f/10 focusing - (a) spectra of forward scattered laser radiation at various gas-jet pressures, and (b) image of the electron beam observed at helium gas density of 4x10^{19} cm^{-3} (gas-jet pressure ~ 60 bar).

aluminium plate kept in front of phosphor screen to stop electrons with energy lower than 5 MeV. The energy spectrum of the electron beam was measured at various plasma densities ranging from about 5x10^{19} cm^{-3} – 1x10^{20} cm^{-3}. The electron energy spectra at three different electron densities (6.5x10^{19} cm^{-3}, 7.5x10^{19} cm^{-3}, and 8.5x10^{19} cm^{-3}) are shown in Fig. 3(a). The typical spectra are continuous with Boltzmann-like [exp(-E/kT$_{eff}$)] distribution. At electron density around 8.5x10^{19} cm^{-3}, in about 20% of the laser shots, highly collimated and mono-energetic electron beam with few tens of pico-coulombs of charge was observed. The spectrum of the mono-energetic electron beam, with peak energy at 21 MeV, is shown in Fig.3(b). The corresponding image of the energy dispersed electron beam is shown in Fig. 3(c). The mono-energetic electron beam had a divergence angle (2θ) in the range of 4–7 mrad, and energy spread (ΔE/E) of ± 4–8%. The resolution (ΔE/E) of the spectrometer at 21 MeV was about 1% and the value reduced at lower energies (0.5% at 10 MeV). The dotted vertical lines in the image represent edges of a slit kept at the entrance of the magnet spectrometer. Due to the large pointing variation of the electron beam which was larger than angular width of the slit, the accuracy of the electron energy measurement was limited. The width of the slit accepts only some of the collimated beams; therefore the monoenergetic electron beam was expected to be produced in more shots than inferred earlier. Although the total beam charge (energy integrated) was few nC, the mono-energetic electron beam had a maximum charge of about 60 pC, carrying about 0.5% of the laser energy.

In the case of f/7.5 focusing, the well collimated electron beam was free from background electrons as shown in Fig. 4(a). A white color dot at the centre of the image was put to represent the laser axis and contours are shown at 5 and 10 degrees from the axis. Fig.4(b) shows the magnified view of the collimated beam. Energy of the collimated beam showed mono-energetic features with

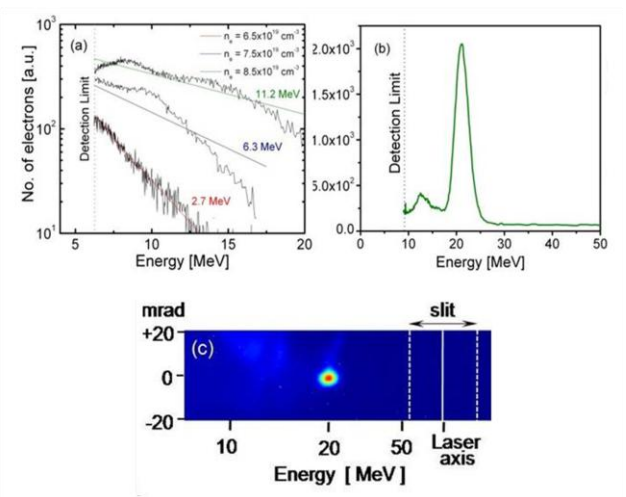

Figure 3: f/10 focusing - (a) continuous energy spectra of accelerated electrons at various plasma densities, (b) mono-energetic spectrum at plasma density of 8.5x10^{19} cm^{-3}, and (c) image of the monoenergetic electron beam after dispersing in the magnetic field

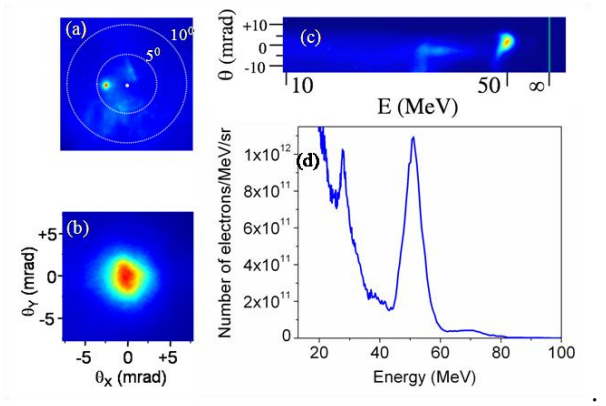

Figure 4: f/7.5 focusing - (a) image of the collimated electron beam, (b) spatial intensity profile of the electron beam, (c) image of energy dispersed mono-energetic electrons, and (d) monoenergetic spectrum of the well collimated electron beam observed at helium gas density of ~ $3x10^{19}$ cm^{-3}.

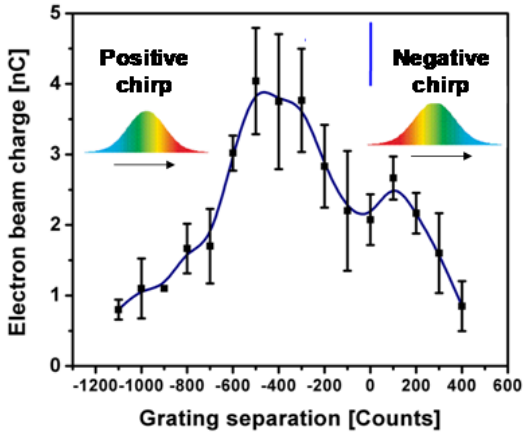

Figure 5: Variation of energy integrated charge of accelerated electrons with laser chirp at plasma density of ~ $5x10^{18}$ cm^{-3} and f/10 focusing.

the peak energy as high as 50 MeV as shown in Fig. 4(c) and (d). The charge contained in the monoenergetic peak was few 10 pC. It may be seen in the Fig. 4(d) that a fraction of electrons gained energy as high as ~ 80 MeV. The high energy electron beam could be produced primarily due to relatively higher intensity of the laser in this case. However, change in size of the focal spot and the background plasma density would also play significant role in laser pulse evolution while propagating in plasma, thereby influencing the injection and acceleration mechanism, as seen in simulations and experiments by other groups [6,7]. The pulse evolution is further modified with the presence of pre-plasma created by nanosecond duration pre-pulse pedestal of main 45 fs intense laser pulse.

The influence of the laser chirp on the electron acceleration was studied by introducing known chirp in the laser pulse through the variation of grating separation of laser pulse compressor. The results had shown that the total charge of the beam can be increased by introducing positive chirp up to certain magnitude as shown in Fig. 5. The observed variation of total charge of accelerated electrons with laser chirp can be understood from the dependence of group velocity [$\upsilon_g = c\,(1-\omega_p/\omega)^{1/2}$] of the laser beam on its wavelength λ, where $\omega = 2\pi\lambda$ [8]. From the expression for group velocity υ_g, it may be noticed that the blue side of the laser pulse travels faster than red side. This results in reinforcement/mitigation of self-modulation process in case of positive chirp/negative chirp. The enhanced self-modulation of the laser pulse will lead to excitation of a larger amplitude plasma wave in the case of positive chirp. Therefore large number of electrons can be injected into the plasma wave. Also higher-order phase dispersive terms associated with optical components in the high power laser systems can cause pulse shape asymmetries with fast rise times of the order of the plasma period for positively chirped laser pulse, which will enhance the growth rate of self-modulation instabilities. These instabilities drive high phase velocity plasma waves, resulting in larger electron yields observed in the experiment [9].

The effect of ASE pre-pulse pedestal on laser propagation in plasma and electron acceleration was studied with f/7.5 focusing. The ASE starts prior to 1 ns before the main laser pulse but this duration can be increased up to about 5 ns. To study the role of pre-pulse shadowgram images of plasma were recorded using a portion of the 45 fs laser beam reaching the interaction region ahead of the main laser beam. The images show [see Fig. 5(a)] clear channel formation by the nanosecond duration pre-pulse pedestal. This plasma channel acts like a waveguide for high intensity main laser beam providing much longer interaction lengths than permitted by Rayleigh length. In the present experiment, the laser beam was guided over 9 times the Rayleigh range under optimal conditions which will be desired for electron acceleration to higher energy. Also, the reduced on-axis plasma density due to the channel formation increases the dephasing length and facilitates higher energy gain as observed in the experiment. The generation of higher energy electrons was found to have strong correlation with the laser guiding channel. It was observed that optimum duration of the pre-pulse is required to form a plasma waveguide. Increase in pre-pulse duration causes refraction of the main laser beam as shown in Fig. 5(b) and the stability of electron beam production gets significantly affected. When the duration was larger than 4 ns, the laser guiding image was not seen and no electron beam was observed. The pointing of the low divergence electron beam with 1 ns duration ASE pre-pulse was found to vary from shot-to-shot but remained within a cone angle of angle of about 5^0 along x- and y-axis as shown in Fig.7. It was found that the electron beam pointing does not correlate with the laser beam pointing variation (which was ~ 100 μrad). Due to the variation in

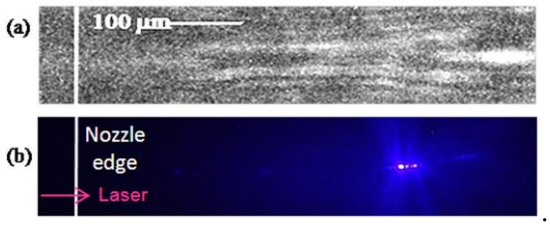

Figure 6: Shadowgram image of the plasma channel formed 1 ns duration ASE pre-pulse pedestal, and (b) strong refraction of the laser beam in plasma channel formed by 3 ns duration pedestal.

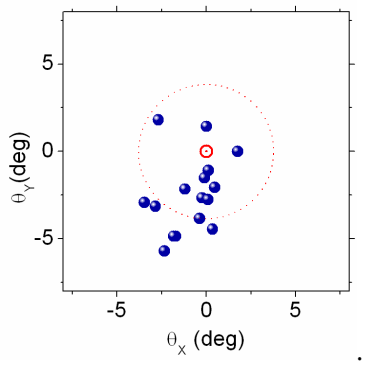

Figure 7: Pointing variation of the well collimated electron beam with f/7.5 focusing and 1 ns duration ASE pre-pulse pedestal.

the beam pointing, for same energy, the location at which beam hits the phosphor screen after passing through the spectrometer varies in the direction of energy dispersion (horizontal direction). Therefore, the shot-to-shot variations in the peak energy of the mono-energetic electron beam may also be due to the pointing variation of the beam. It was observed by Mangles *et al* [9] that the pointing stability of the electron beam could be improved by reducing the intensity of the ASE pre-pulse pedestal.

In summary, we have produced mono-energetic electron beams with energy in the range of 10 – 50 MeV for laser-plasma based electron acceleration. Laser focusing with lower f-number produces mono-energetic electron beam at lower gas density suitable for high energy electron acceleration. The well collimated electron beam produced at lower density would be of practical interest as it does not contain background electrons. Introducing positive chirp increases the growth rate of self-modulation and produces higher electron yield. The use of laser pre-pulse provides a simple method to produce guiding channel for intense laser beam. However, shot-to-shot variation in the pre-pulse intensity can change the cavity structure and electron beam parameters. If the level of pre-pulse is controlled, the method may be useful for producing few 100 MeV energy, stable electron beam from longer plasma channels. In future experiments with the 10 TW laser, we will aim to improve the stability the monoenergetic electron beam. In this direction, we will explore the use of high-Z gas-jet targets or reduce the pre-pulse intensity below the plasma formation threshold using saturable absorbers or plasma mirrors. For higher energy acceleration up to GeV or more, centimetre long plasma channels would be required. Such long plasma channels could be produced with the use of laser triggered capillary waveguide structures. We have studied the discharge characteristics of such capillary columns. These capillary waveguides will be characterized for ultra-high intensity laser beam guiding. They will be subsequently used for GeV electron acceleration with the 150 TW laser facility to be installed later this year. By focusing the 150 TW laser beam using longer f-number optics on gas-jet targets, it is expected that the stability of the electron beam will be improved. These beams may then be used for generating x-rays from inverse Compton scattering or from undulating magnetic fields.

The authors would like to acknowledge support from S.R. Kumbhare, R.P. Kushwaha, and S. Sebastin in setting up the experiment and R.A. Khan, R.K. Bhat and R.A. Joshi in operating the Ti:sapphire laser, and C.P. Navathe and his team for electronics support.

REFERENCES

[1] T. Tajima and J. M. Dawson, Phys. Rev. Lett. 43 (1979) 267.

[2] E. Esarey, C. B. Schroeder, and W. P. Leemans, Rev. Mod. Phys. 81 (2009) 1229.

[3] B. S. Rao, P. A. Naik, V. Arora, H. Singhal, U. Chakravarty, R. A. Khan, P. D. Gupta, K. Nakajima, and T. Kameshima, IEEE Trans. Plasma Sci. 36, (2008) 1694.

[4] Hosokai T, Kinoshita K, Watanabe T, Yoshii K, Ueda T, Zhidkov A and Uesaka M, 2002 *Proc. 8th European Particle Accelerator Conf. (EPS)* p 981

[5] B. S. Rao, A. Moorti, P. A. Naik, and P. D. Gupta, New J. Phys. 12 (2010) 045011.

[6] A. Pukhov and J. Meyer-ter-Vehn, Appl. Phys. B 74 (2002) 355.

[7] J. Faure, Y. Glinec, G. Gallot, and V. Malka, Phys. Plasma 13 (2006) 056706.

[8] T.-W. Yau, C.-J. Hsu, H.-H. Chu, Y.-H. Chen, C.-H. Lee, J. Wang, S.-Y. Chen, Phys. Plasmas 9 (2002) 391.

[9] C. B. Schroeder, E. Esarey, C. G. R. Geddes, Cs. Toth, B. A. Shadwick, J. van Tilborg, J. Faure, and W. P. Leemans, Phys. Plasmas 10 (2003) 2039.

[10] S. P. D. Mangles, A. G. R. Thomas, M. C. Kaluza, O. Lundh, F. Lindau, A. Persson, Z. Najmudin, C.-G. Wahlstrom, C. D. Murphy, C. Kamperidis, K. L. Lancaster, E. Divall, and K. Krushelnick, Plasma Phys. Control. Fusion 48 (2006) B83.